Cellulose (2022) 29:1807–1820
https://doi.org/10.1007/s10570-021-04389-2

ORIGINAL RESEARCH

Investigating the adsorption behavior and mechanism of Eu(III) and Au(III) on β-cyclodextrin/polyethylenimine functionalized waste paper

Fenglei Liu · Shan Hua · Qingyuan Hu · Chao Wang · Baowei Hu

Received: 9 September 2021 / Accepted: 17 December 2021 / Published online: 29 January 2022

Abstract A bio-adsorbent (DAWP-PEI-β-CD) was facilely prepared by introducing polyethylenimine (PEI) and β-cyclodextrin (β-CD) into dialdehyde waste paper (DAWP) via a facile two-step method. The structures, morphologies and compositions of the as-prepared adsorbents were characterized by Fourier transform infrared spectroscopy (FT-IR), X-ray diffraction (XRD), scanning electron microscopy (SEM), solid state nuclear magnetic resonance spectrometry (NMR) and X-ray photoelectron spectroscopy (XPS) techniques. Results showed that the pH values, adsorption temperature and contact time played a vital role in uptake of Eu(III) and Au(III). Meanwhile, the adsorption behavior of Eu(III) and Au(III) could be fitted felicitously with the Langmuir and the pseudo-second-order models, and the maximum adsorption capacities of Eu(III) (pH = 6.0) and Au(III) (pH = 2.0) onto DAWP-PEI-β-CD were 424.2 and 241.3 mg/g, respectively. Further advanced spectroscopy analysis revealed that the elimination of Eu(III) was attributed to host-guest inclusion and surface complexation interaction, while adsorption of Au(III) might stem from a combination of electrostatic attraction, chelation, host-guest inclusion and redox interaction. This study demonstrated that DAWP-PEI-β-CD was a promising environmental functional material to separation and enrichment of Eu(III) and Au(III) from contaminated water.

Supplementary Information The online version contains supplementary material available at https://doi.org/10.1007/s10570-021-04389-2.

F. Liu · S. Hua · Q. Hu · B. Hu (✉)
School of Life Science, Shaoxing University, Huancheng West Road 508, Shaoxing 312000, People's Republic of China
e-mail: hbw@usx.edu.cn

C. Wang
School of Environment, Tsinghua University, Beijing 100084, People's Republic of China

Graphical abstract

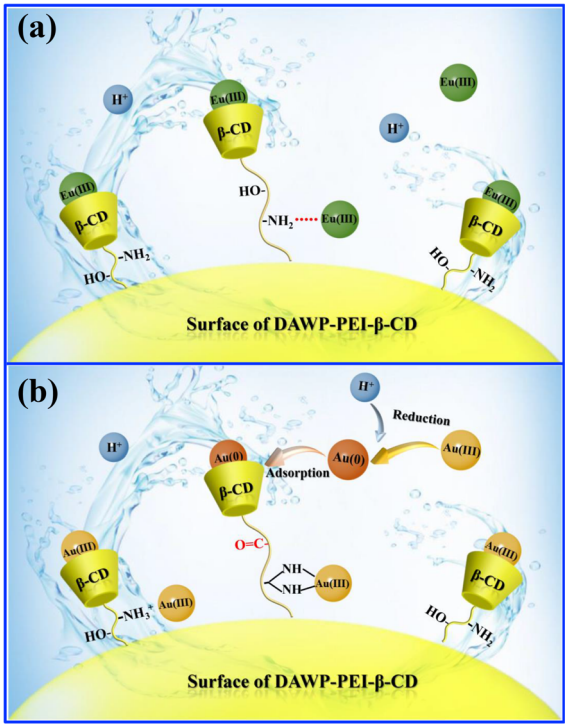

Keywords Waste paper · β-CD · Eu(III) · Au(III) · Adsorption

Introduction

With the rapid promotion of urbanization, the radionuclides and precious metals pollution have become an imperative global environmental problem, especially for europium (Eu) and Aurum (Au) (Zhao et al. 2015a, b). Generally, europium has major applications in neutron protection, laser, and atomic energy industry field, while gold is widely used in the fields of industry, agriculture, and medicine (Neri et al. 2021; Zhao et al. 2021a, b). However, a large amount of wastewater containing Eu(III) or Au(III) is produced in the process of application. Thereby, how to efficiently eliminate the Eu(III) and Au(III) ions from the polluted water sources or industrial wastes to avoid these pollutants migration and transformation is a very pressing issue. In an effort to handle those challenges, several state-of-the-art techniques have been proposed to purify Eu(III) or Au(III)-containing wastewater, such as chemical precipitation (Yan et al. 2019), membrane processing (Wang et al. 2020), electrolysis (Liu et al. 2019a, b) and adsorption (Zhao et al. 2019). Among them, adsorption seems to be one of the most effective and practical technologies owing to its simplicity and flexibility features. Nowadays, different types of adsorbents have been developed and evaluated for Eu and Au ions clean-up, such as carbon nanotubes (Chen et al. 2008), graphene oxide (Ma et al. 2019), viscose fiber (Liu et al. 2020a, b), corn starch (Liu et al. 2019a, b) and MOFs (Zhang et al. 2021a, b). However, these solid materials generally have the defects of low adsorption amounts, long equilibrium time and weak stability under various environmental conditions. One suggested approach is to the preparation of new materials with high adsorption capacity and high chemical stability, so that it can be used to efficient eliminate the two contaminant classes from wastewater.

Recently, biomass materials have stimulated researchers' interest on account of their renewable, contamination-free, and low-cost characteristics (Zhu et al. 2021). So far, different types of bio-materials have been applied to eliminate the radionuclide and precious metal ions from the wastewater stream, such as tannin (Liu et al. 2021a, b, c), chitosan (Liu et al. 2021a, b, c) and cellulose (Zhang et al. 2021a, b). Indeed, β-cyclodextrin (β-CD) is also an inexpensive sustainable biomass resource, which is mainly produced from the enzymatic degradation of starch. More importantly, β-CD is a cyclic oligosaccharide formed by seven α-D-glucose units [small-caps "D"] linked by α-1,4-glycosidic bonds. It has been proven to perform well in wastewater treatment (Crini et al. 2021). However, β-CD requires a process of immobilization/insolubilization before being used as an adsorbent for aqueous phase applications due to its water solubility. To compensate for this disadvantage, many efforts have been made to immobilize β-CD onto various water-insoluble matrices. For instance, Zhao et al. (2016) developed an EDTA-β-cyclodextrin material to preconcentrate the Eu(III) ions from simulated seawater, and the maximum adsorption capacities reached up to 0.365 mmol/g. Martin-Trasanco et al. (2017) reported a β-cyclodextrin polymer to selective recovery of Au(III) from acid medium, and it was observed that Au(III) ions could be efficiently reduced to gold nano-particles by hydroxyl groups. Guo et al.

(2015) synthesized a Fe_3O_4@cyclodextrin magnetic composite via a simple chemical co-precipitation method, and this magnetic composite could efficiently remove Eu(III) from industrial wastewater. Kyrychenko et al. (Slavgorodska and Kyrychenko 2020) explored the adsorption behavior of β-cyclodextrin onto gold nano-particles, and it was found that β-CD binding onto the AuNP surface occurred through multiple non-covalent interactions. However, although these surface modification strategies could effectively immobilize β-CD on insoluble carrier, most of these methods used complicated procedures and toxic reagents. More importantly, the majority of the previously reported β-CD based adsorbents suffered from the low adsorption amounts and slow reaction rates toward the targeted contaminants. Consequently, there is an urgent need to propose a new β-CD immobilization strategy to elimination of the targeted pollutants. It is worth noting that waste paper (WP) is an inexpensive, renewable, and massively available material, of which the main components are cellulose and hemicellulose. Notably, WP is easy to be oxidized by strong oxidant, which can produce a large amount of aldehyde groups on its skeleton. Furthermore, the aldehyde groups can form covalent and hydrogen bonds with the amine and hydroxy functional groups under the mild environmental conditions. Polyethylenimine is a kind of sterically branched polymer with larger numbers of amino groups, such as primary, secondary, and tertiary amine groups. And one third of the atoms of PEI are protonatable amino nitrogen atoms, which exhibit high affinity towards metal ions (Zhao et al. 2017). Hence, the special chemical structure of DAWP opens up an opportunity for the facile introduction of β-CD and PEI through one step or two-step synthetic strategies.

The purposes of this study were: (1) to develop a novel bio-adsorbent (DAWP-PEI-β-CD) via a facile two-step method and investigate its adsorption performance towards Eu(III) and Au(III) under various environmental conditions; (2) to characterize the as-synthesized bio-adsorbents by different physicochemical and spectroscopic techniques (FT-IR, XRD, SEM, NMR, XPS); (3) to evaluate the adsorption property of Eu(III) and Au(III) on DAWP-PEI-β-CD using the kinetic and isotherm models; (4) to understand the interaction mechanism between DAWP-PEI-β-CD and Eu(III)/Au(III) ions. This study will provide new clues to the overall recycling of Eu(III) and Au(III) in environmental pollution treatments.

Materials and methods

Materials and reagents

β-Cyclodextrin (β-CD, 98%), polyethyleneimine (PEI, M.W.600, 99%), epichlorohydrin (EPI, AR), $Eu(NO_3)_3.6H_2O$ (99.9%) and $HAuCl_4{\cdot}4H_2O$ (99.9%) were purchased from Sinopharm Reagent Co. Ltd., China. The NaCl (99.5%), $FeCl_2$ (98%), $NaIO_4$ (99.5%), NaOH (95%), HCl (37%), $CuCl_2$ (98%), $ZnCl_2.7H_2O$ (98%), $NiCl_2{\cdot}6H_2O$ (99.9%), $FeCl_3{\cdot}6H_2O$ (99%) and $K_2Cr_2O_7$ (98%) were received by Shanghai Macklin Biochemical Co., Ltd. Waste paper (WP) was obtained from personal laboratory and crushed into small pieces mechanically before use.

Preparation of DAWP-PEI-β-CD

The preparation process of bio-adsorbent (DAWP-PEI-β-CD) was proposed as Fig. 1, and the detailed preparation procedure with minor modification according to references (Rahman et al. 2021; Zhao et al. 2015a, b). Firstly, 2 g of waste paper and 60 mL of sodium periodate solution (pH=4.0, 0.7 mol/L) were added into 500 mL of round-bottom flask under stirring conditions. Then, the mixtures were stirred at 313 K for 5 h under exclusion of light, and the oxidized waste papers were obtained and named as DAWP. Secondly, 1 g of DAWP was added into 50 mL of PEI solution (5 wt%) to form a suspension, which was continuously stirred at room temperature for 12 h to acquire yellow solids (DAWP-PEI). Finally, 4.8 g of EPI and 10 g of β-CD were dissolved into 100 mL of NaOH solution (7 wt%). And then 2 g of DAWP-PEI was joined with the modification solution under intense stirring for 6 h. After that, the mixture was filtered with ultra-pure water to make it neutral, and the as obtained bio-adsorbents (DAWP-PEI-β-CD) were dried in an oven for further use.

Characterization

The Fourier transform infrared spectrometer (FT-IR) spectra were analyzed on the NEXUS 870 spectroscopy (Thermo, Madison, USA). X-ray

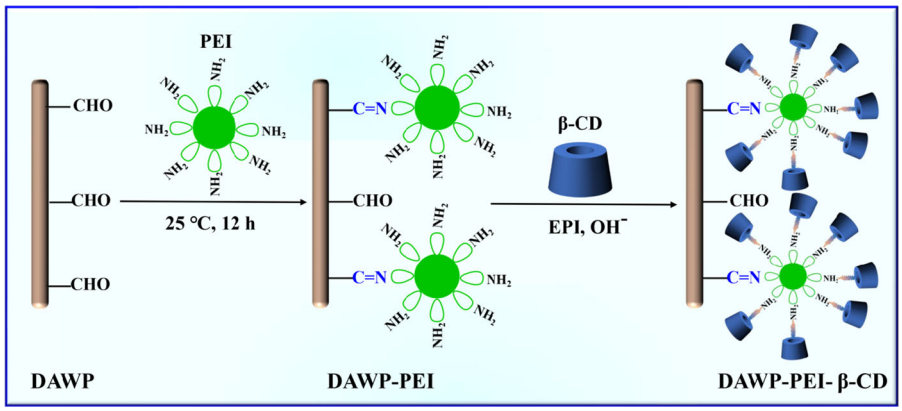

Fig. 1 Schematic diagrams for the synthetic procedures of DAWP-PEI-β-CD

photoelectron spectroscopy (XPS) data were registered in an ESCALAB 250 XPS (ThermoFisher, AlKa). The morphological analysis was carried out by scanning electron microscope (SEM) using a QUANTAFEG 400 (FEI company, USA), and elemental mapping was performed by Thermo Scientific Ultra Dry SDD Energy-dispersive X-ray spectroscopy (EDS, USA). The X-ray diffraction (XRD) analysis was performed on a Rigaku TTRIII diffraction (Japan) with Cu Kα irradiation over a 2θ range from 10° to 90°. Solid state nuclear magnetic resonance spectrometry (NMR) was recorded on a Bruker AVANCE II 400WB spectrometer (Germany). The surface charge density of samples was determined by a Malvern Instruments Zetasizer Nano ZS90 (England).

Batch removal experiments

Batch experiments were carried out to explore the adsorption performance of Eu(III) and Au(III) on DAWP-PEI-β-CD. Here, 10 mg of DAWP-PEI-β-CD was added into 50 mL of known concentration Eu(III) or Au(III) solution with the desired pH values. Then, the suspensions were shaken in the incubator at 250 rpm for 24 h until adsorption equilibrium. Upon the completion, the solid adsorbents were separated from solution phase by centrifugation. Subsequently, the supernatant concentration of Eu(III) was analyzed by the UV-vis adsorption spectrometer at the wavelengths 652 nm, while the residual concentration of Au(III) was measured by ICP-AES. The adsorption ability of DAWP-PEI-β-CD was performed by transferring 10 mg of bio-adsorbents into 50 mL of targeted pollutants, which already contained a series of different concentrations of Eu(III) and Au(III) solution. The kinetic experiment of Au(III) and Eu(III) on DAWP-PEI-β-CD were carried out at optimal pH values, and the concentrations of metal ions were measured and recorded at different time points until adsorption equilibrium. The adsorbed amounts of Eu(III) and Au(III) onto DAWP-PEI-β-CD were calculated from the difference of the initial concentration and the final concentration remained in solution after equilibrium.

Results and discussion

Adsorbent characterization

XPS analyses were used to investigate the surface chemical compositions of DAWP, DAWP-PEI and DAWP-PEI-β-CD. As shown in Fig. 2, the C1s spectrum of DAWP could be quantitatively resolved into three bonds at 284.81, 286.62 and 288.12 eV corresponded to carbon-carbon bond (C-C), carbon-oxygen bond (C-OH) and carbon -oxygen double bond (C=O), respectively. Interestingly, once the PEI molecules were immobilized on DAWP via Schiff base reaction, two new peaks appeared at 287.15 eV (C=N) and 285.74 eV (C-N), proving that a mass of amino groups existed on the surface of DAWP-PEI (Liu et al. 2020a, b). However, as the β-CD molecules were further introduced into DAWP-PEI through cross-linking reaction, the relative content of C-N on DAWP-PEI (14.20%) was lower than that of DAWP-PEI-β-CD (25.58%), and other characteristic peaks were still presented in DAWP-PEI-β-CD. These

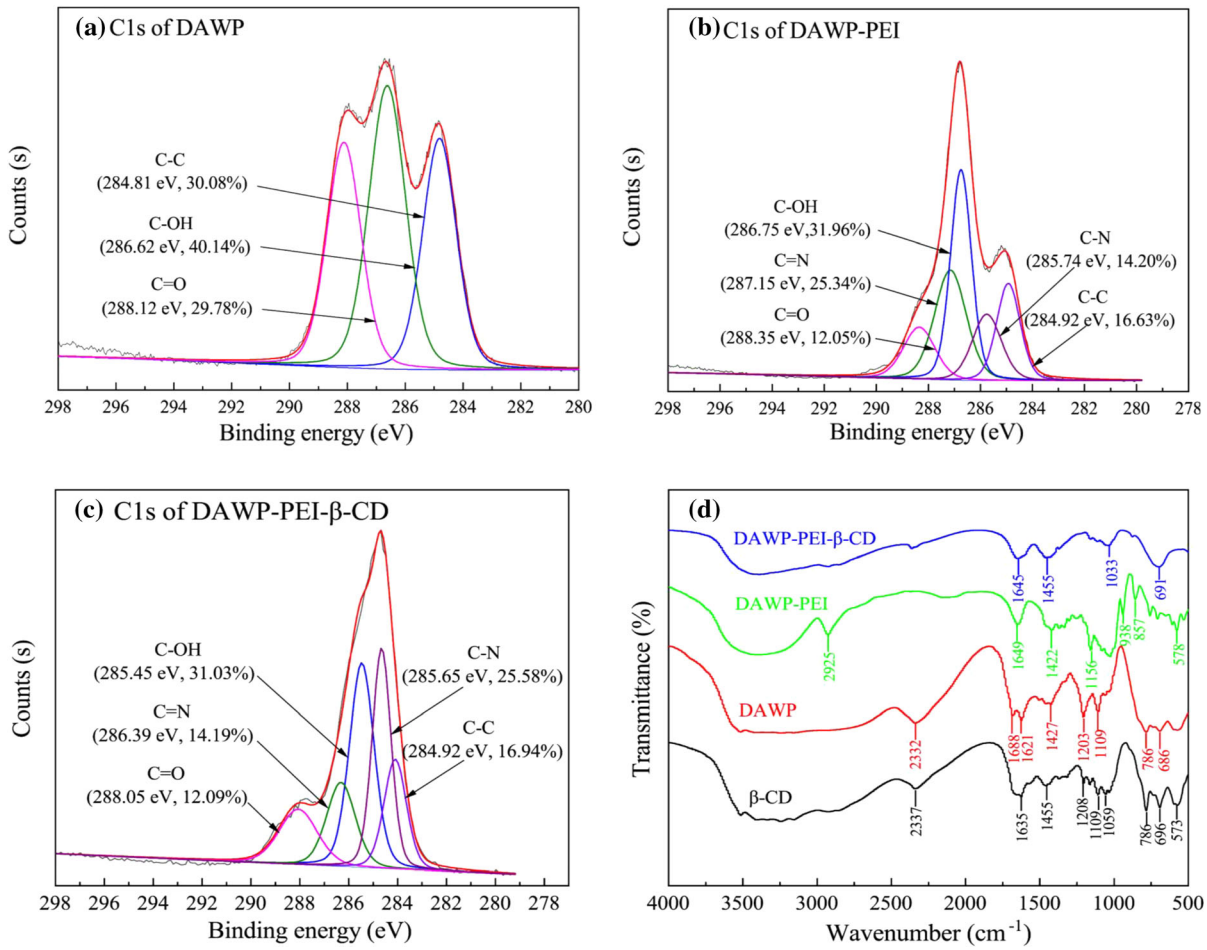

Fig. 2 XPS C1s spectrum (**a–c**) and FT-IR (**d**) of β-CD, DAWP, DAWP-PEI and DAWP-PEI-β-CD

observations confirmed that PEI and β-CD molecules had been successfully immobilized on DAWP via a facile two-step method.

FT-IR measurements were mostly used in order to confirm the formation of functional groups. Thus, different functional groups were detected in the IR spectra of β-CD, DAWP, DAWP-PEI and DAWP-PEI-β-CD. In Fig. 2d, the typical peaks of β-CD at 3352 cm^{-1} and 1208 cm^{-1} were generated by the -OH and -CH_2 bending vibrations, whereas another band at 1059 cm^{-1} was produced by inverse-symmetric glycosidic (Wang et al. 2014). The bands centered at 1688 cm^{-1}, 1427 cm^{-1} and 1109 cm^{-1} ascribed to –C=O, –CH_2 and C–O–C stretching vibrations of DAWP, respectively (Liu et al. 2019a, b). Notably, once the PEI molecules were introduced into oxidized waste paper, two regular peaks appeared at 1649 cm^{-1} and 1422 cm^{-1} corresponded to –C=N and –NH_2, respectively (Al-Harahsheha et al. 2020). Interestingly, after the cross-linking reaction, the characteristic peaks of β-CD and PEI were also appeared in the IR spectra of DAWP-PEI-β-CD, such as primary amine (1455 cm^{-1}) and the b(1-4) skeleton vibrations (1033 cm^{-1}). These analysis results further proved that the β-CD and PEI were successfully introduced into the oxidized waste paper.

The chemical structure of all adsorbents was further assessed by solid state NMR measurements. In Fig. 3, one can see that the broad signals from 102 ppm to 59 ppm were attributed to the carbon atoms in β-CD, and the signals at δ = 63, 72, 84 and 102 ppm corresponding to C-d, C-a, C-e and C-b, respectively (Shen et al. 2015). Compared with β-CD, the characteristic peaks of carbon atoms at δ = 72 ppm (C-2) and 65 ppm (C-4)

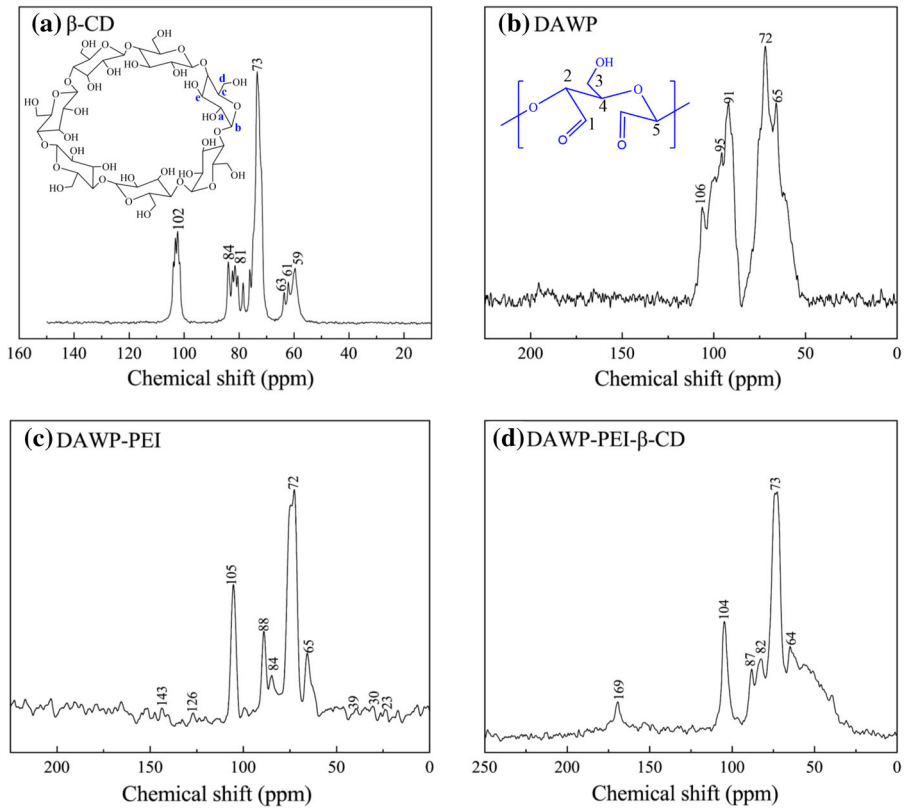

Fig. 3 ^{13}C NMR spectra of β-CD, DAWP, DAWP-PEI and DAWP-PEI-β-CD

were almost overlapped or disappeared in the NMR spectrum of DAWP, which may be related to the signal amplification of C-5 and C-3 after oxidation reaction. However, when DAWP was reacted with PEI, there were several new characteristic peaks appeared at the NMR spectra of DAWP-PEI. For instance, the carbon-nitrogen double bond (C=N) as well as carbon-nitrogen single bond (C-N) were observed at δ = 143 ppm and 30 ppm, respectively. Interestingly, most of DAWP and PEI's carbon atom signals were also detected on the NMR spectra of DAWP-PEI-β-CD after cross-linking reaction, and a different signal appeared at δ 169 ppm may be ascribed to C=O. These results were in accordance with FT-IR and XPS results, which further manifested that the successful cross-linking between DAWP and β-CD/PEI.

Influences of pH values

As is well-known, solution pH not only can affect the relative distribution of pollutants species but also change the surface charge of adsorbents. Thus, the adsorption performance of DAWP-PEI-β-CD towards Eu(III) and Au(III) were investigated in this work. As depicted in Fig. 4a, adsorption amounts of Eu(III) on DAWP-PEI-β-CD were up to 282 mg/g rapidly from 2.0 to 5.0, subsequently maintained the high level within pH the range of 6.0-9.0, which implied that solution pH played a vital role in elimination of contaminants. This phenomenon could be explained by the relative distribution of Eu(III) species and the surface charge of DAWP-PEI-β-CD. It was reported that Eu(III) ions were mainly presented as Eu^{3+} species at pH<5.0 in water solution, and then $Eu(OH)^{2+}$ and $Eu_2(OH)_2^{4+}$ species began to increase with pH further increasing (Li et al. 2020). Meanwhile, zeta potential analyzer determined the surface charge density of DAWP-PEI-β-CD was 3.29 (Fig. S1). Thus, according to Coulomb's law, the positive charge of Eu(III) species was more easily adsorbed on the negatively charged DAWP-PEI-β-CD through electrostatic attraction. However, the adsorption behavior of Au(III) was significantly different from that of

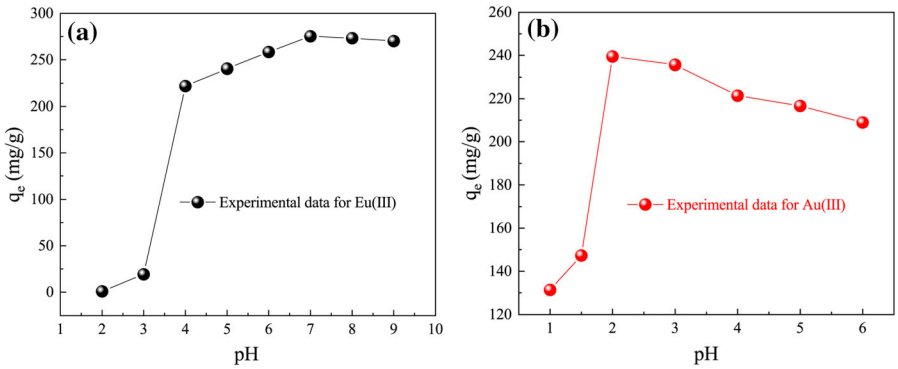

Fig. 4 Effect of initial pH on elimination of Eu(III) and Au(III) by DAWP-PEI-β-CD

Eu(III) at various pH values. In Fig. 4b, one can see that the adsorbed amounts of Au(III) on DAWP-PEI-β-CD increased sharply as pH values were raised from 1.0 to 2.0, and then sharply decreased over the pH range 2.0–6.0. Such a pH-dependent adsorption can be explained from the point of view of the following aspects. At lower pH values, the Au(III) ions mainly existed as $AuCl_4^-$, which were favorable to capture on the positively-charged DAWP-PEI-β-CD via electrostatic interactions. Notably, the chloride ion occupied a part of the active sites during adsorption process at pH < 2.0, which led to lower adsorption amounts (Wang et al. 2015). However, under high pH conditions, the negative charge increased on the surface of DAWP-PEI-β-CD and the electrostatic repulsion would occur between the bio-adsorbents and adsorbates at high pH values.

Adsorption isotherms and thermodynamic studies

The adsorption isotherms are an important factor in understanding the adsorption efficiency and studying the adsorption mechanism. Figure 5 displays the relationship between the residual Eu(III) and Au(III) concentrations and the equilibrium adsorption capacities on DAWP-PEI-β-CD at room temperature. Evidently, along with the initial concentration increasing, the adsorption amounts of Eu(III) and Au(III) on DAWP-PEI-β-CD rapidly increased at the beginning, and then tended to adsorption equilibrium. Interestingly, the equilibrium adsorption capacities of Au(III) were both higher than that of Eu(III) on DAWP-PEI and DAWP-PEI-β-CD, which was evident that the greater affinity to Au(III) than Eu(III) in the adsorption process. To determine the saturated adsorption amounts and adsorption type, the Langmuir and Freundlich equations were applied to fit the experimental data, and the detailed fitting results were provided in Fig. 5 and Table S1. As expected, the results of calculation and simulation showed that the adsorption behavior of Eu(III) and Au(III) were fitted well by the Langmuir model, which indicated that adsorption of the two targeted contaminants onto DAWP-PEI-β-CD surfaces was localized in a monolayer (Yang et al. 2019; Dai et al. 2019; Wu et al. 2019). Besides, the adsorption thermodynamics of Eu(III) and Au(III) on DAWP-PEI-β-CD were also measured using the Gibbs equations. As listed in Table S2, the spontaneous and endothermic adsorption processes were revealed by the negative ΔG° and positive ΔH° values, whereas the positive ΔS° reflected a decrease in the randomness during the adsorption process. Notably, the maximum uptake amounts of DAWP-PEI-β-CD for single Eu(III) and Au(III) were 241.3 and 424.2 mg/g, which were far higher than that of the reported available materials (Table 1). Such a high adsorption amount could be ascribed to the special chemical structure and the large cavities, which were advantageous for accommodating more Eu(III) and Au(III).

Adsorption kinetics

Adsorption kinetics not only focuses on the relationship between adsorption capacity and adsorption time, but also evaluate the rate of the interaction process. Figure 6 illustrates the time-dependent experiments of Eu(III) and Au(III) adsorbed onto DAWP-PEI-β-CD. As excepted, the concentration of targeted contaminants rapidly declined during the initial phase, and

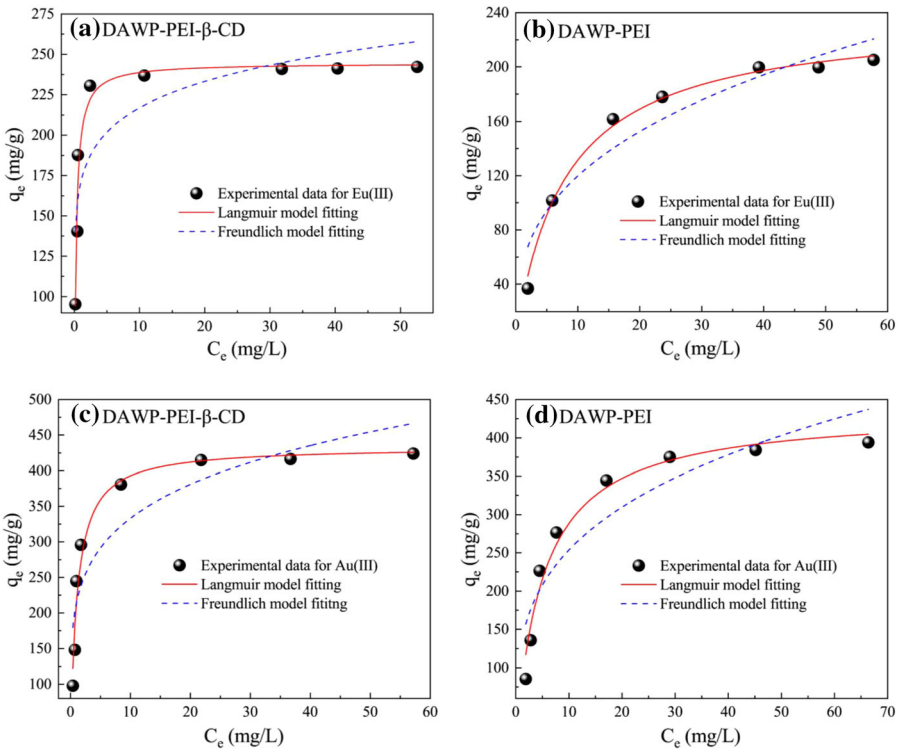

Fig. 5 Adsorption isotherms of Eu(III) and Au(III) on DAWP-PEI and DAWP-PEI- β-CD as well as fitting by the Langmuir and Freundlich equations

Table 1 Comparison of Eu(III) and Au(III) elimination by DAWP-PEI-β-CD and other adsorption materials

Sorbents	Adsorption capacity (mg/g)		References
	Eu(III)	Au(III)	
DAWP-PEI-β-CD	241.3	424.2	This work
Graphene oxide	83.5	–	Ma et al. (2019)
Viscose fiber	–	535	Liu et al. (2020a, b)
EDTA-β-CD	55.2	–	Zhao et al. (2016)
Tannin acid	–	298.5	Liu et al. (2019a, b)
Fe_3O_4/PDA	151.1	–	Fang et al. (2017)
Resin	–	920	Chen et al. (2020)
Al_2O_3	5.14	–	Sun et al. (2012)

then tended to a constant value with the extension of incubation time. The rapid adsorption in the beginning may be due to the greater concentration gradient and more available sites for adsorption. Subsequently, the active sites were gradually depleted, resulting in the final adsorption equilibrium. Note that the Au(III) exhibited faster kinetics compared with Eu(III) at optimal water environmental condition, which suggested that Eu(III) ions took a relatively longer time to diffuse into the interlayer of DAWP-PEI-β-CD. To figure out the adsorption rate and rate determining step, different kinetic models were applied to simulate the kinetic data, and the corresponding fitting curves and parameters were displayed in Fig. 6 and Table S3. According to the fitted results, one can see that the pseudo-first-order equation either overestimated or underestimated the kinetics behavior of Eu(III) and Au(III) on DAWP-PEI-β-CD, while the pseudo-

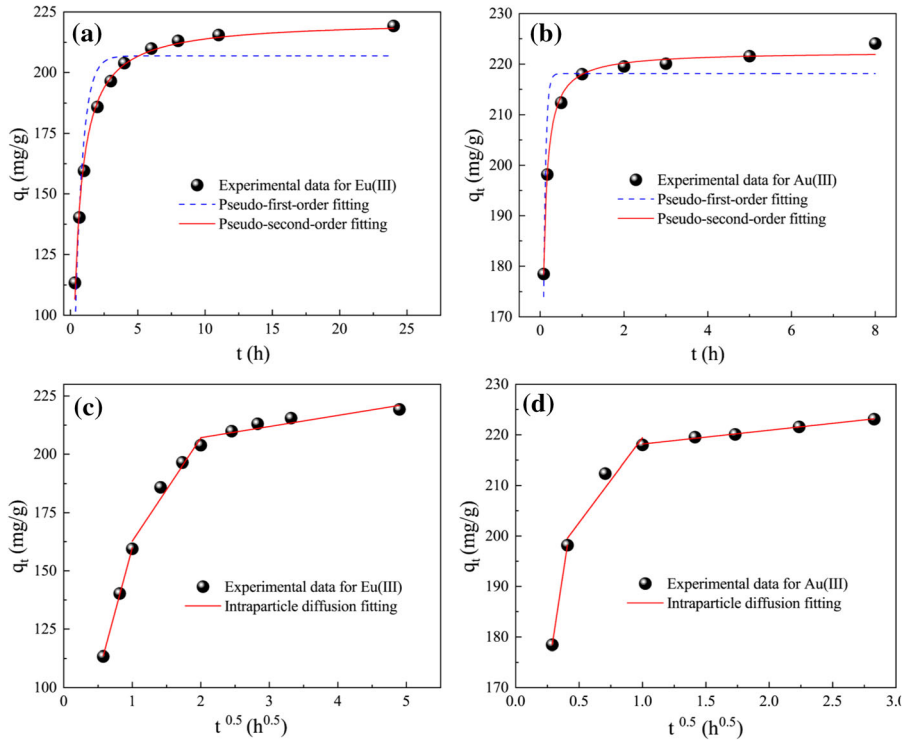

Fig. 6 Effects of the equilibrium time on Eu(III) and Au(III) adsorbed on DAWP-PEI-β-CD as well as modeling by different kinetics equations

second-order model could well simulate the kinetic process from the beginning to the end, and the calculated limits of quantification were close to the experimental limits of quantification, which implied that adsorption of the two targeted pollutants mainly depended on chemical adsorption (Cheng et al. 2018; Wang et al. 2019). To further identify the main rate-controlling step, the kinetic data were further analyzed by the Intraparticle diffusion equation, and the plots of qt versus $t^{1/2}$ were displayed in Fig. 6c, d. The simulation results exhibited that the lines did not pass through the origin and tended to be multilinear, which manifested that the rate controlling steps did not only include intraparticle diffusion, and other reactions (Qiu et al. 2020; Hu et al. 2021; Yin et al. 2020).

Selectivity test

Considering the practical application of the targeted pollutants removal from industrial wastewater, the effect of competing ions on adsorbents was also important. Thus, the adsorption selectivity of DAWP-PEI-β-CD towards Eu(III) and Au(III) was investigated in a mixed system, in which the concentration of metal ions was all controlled at 50 mg/L. In Fig. S2, one can see that the adsorption capacity of Au(III) on DAWP-PEI-β-CD was calculated as 209 mg/g in a single system, and that was reduced by 20.1% in a mixed system. This phenomenon occurred due to most of co-existing metal ions existed as their cationic or neutral forms, while Au(III) ions were mainly existed as $AuCl_4^-$ in acidic solution. Thus, the negatively charged Au(III) species could occupy more adsorption sites on the surface of DAWP-PEI-β-CD, which led to a high Au(III) adsorption amounts. Besides, it should be pointed out that the molecular structure of Eu(III) was similar to that of Au(III) to some extent, but the removal amounts of Eu(III) was still lower than that of Au(III) at this adsorption conditions. This may be due to the electrostatic repulsion occurred between Eu(III) ions during adsorption process. This result manifested that DAWP-PEI-β-CD exhibited high selectivity for Au(III) against other co-existing pollutants in the multi-solute system.

Elimination mechanisms

To find out the detailed elimination mechanism, the as-prepared bio-adsorbent's surface properties and specific elemental constitutes were explored by SEM, XPS and XRD after binding with Eu(III) and Au(III). In Fig. 7, one can see that the main components of DAWP-PEI-β-CD were C, H, N and O, whereas the element Eu and Au were spread over the whole surface of DAWP-PEI-β-CD-Eu and DAWP-PEI-β-CD-Au, suggesting that DAWP-PEI-β-CD could efficient separation of Eu(III) and Au(III) from water environment. Interestingly, in Fig. 8a, in addition to C1s and O1s, the spent DAWP-PEI-β-CD's surface also appeared characteristic peaks of Eu3d and Au4f, which was consistent with the results analyzed in EDS, further proved that the successful immobilization of the two targeted pollutants onto DAWP-PEI-β-CD.

To resolve the chemical properties and states of Eu and Au atoms on the DAWP-PEI-β-CD, the high-resolution spectra of Eu3d and Au4f were further resolved by deconvolution method. In Fig. 8b, one can see that two main peaks located at 1134.49 eV ($Eu3d_{3/2}$) and 1164.16 eV ($Eu3d_{5/2}$) in the high-resolution Eu3d spectrum corresponded to the Eu(III) signals, which implied that only Eu(III) ions existed on the surface of DAWP-PEI-β-CD, and the surface complexes reaction dominated the processes of Eu(III) uptake on DAWP-PEI-β-CD (Huang et al. 2018). However, in Fig. 8c, the Au4f peak mainly consisted of $Au4f_{7/2}$ and $Au4f_{5/2}$, each of which could be further divided into Au(III) and Au(0). Specifically, the peaks at 83.36 eV ($Au4f_{7/2}$) and 87.08 eV ($Au4f_{5/2}$) corresponded to Au(III), whereas the signatures at 84.18 eV ($Au4f_{7/2}$) and 89.05 eV ($Au4f_{5/2}$) were ascribed to Au(0), which demonstrated that a large amount of Au(0) existed onto the surface of spent bio-adsorbents (Pestov et al. 2015). This result was further proved by the XRD analysis. In Fig. 8e, one can see that the powder XRD patterns of DAWP-PEI-β-CD exhibited two major peaks at 2θ = 12.3° and 18.1°, which may be ascribed to the characteristic peak of β-CD. However, after adsorption of Au(III), there were four the high intensity peaks appeared at the XRD patterns of DAWP-PEI-β-CD-Au. The reflections of elemental gold were observed at 2θ = 38.19°, 44.38°, 64.71° and 77.52° with the corresponding planes of (111), (200), (220) and (311). Noticeably, the specific area percentage of C=O enhanced from 12.09 to 15.78%, and the content of Au(0) reached up to 54.65% after adsorption of Au(III) (see Table S4). These phenomena illustrated that part of surface adsorbed Au(III) had been reduced to Au(0) during the Au(III) capture

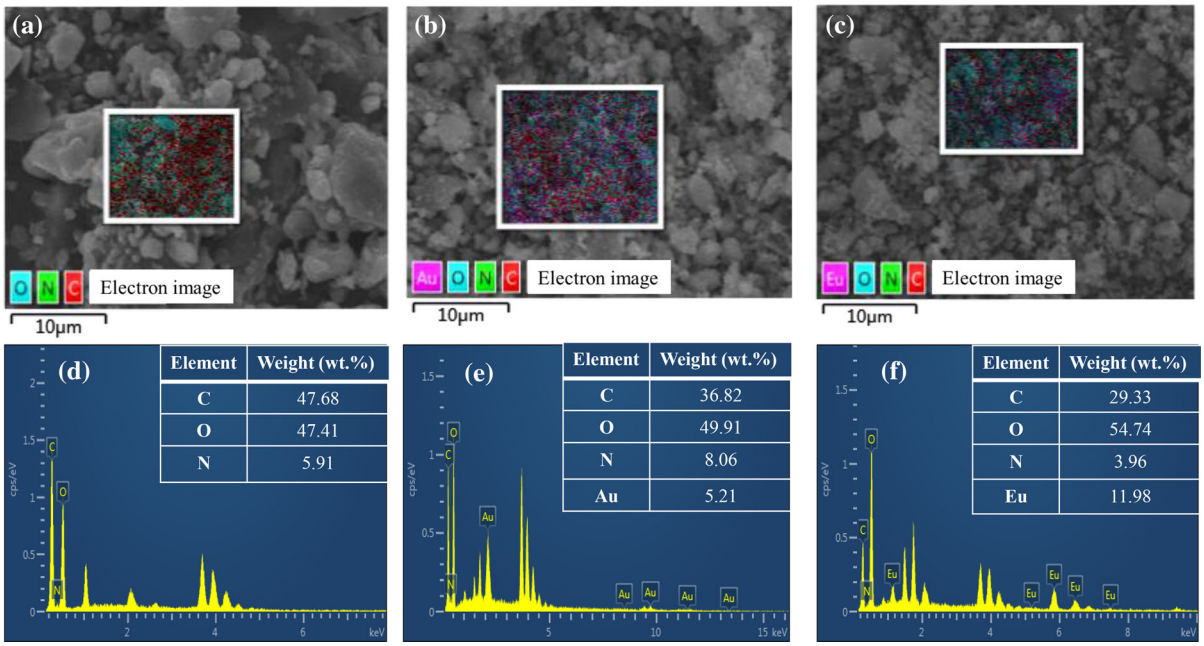

Fig. 7 The SEM images and EDS spectrum of DAWP-PEI-β-CD (**a**, **d**), DAWP-PEI-β-CD-Au (**b**, **e**) and DAWP-PEI-β-CD-Eu (**c**, **f**)

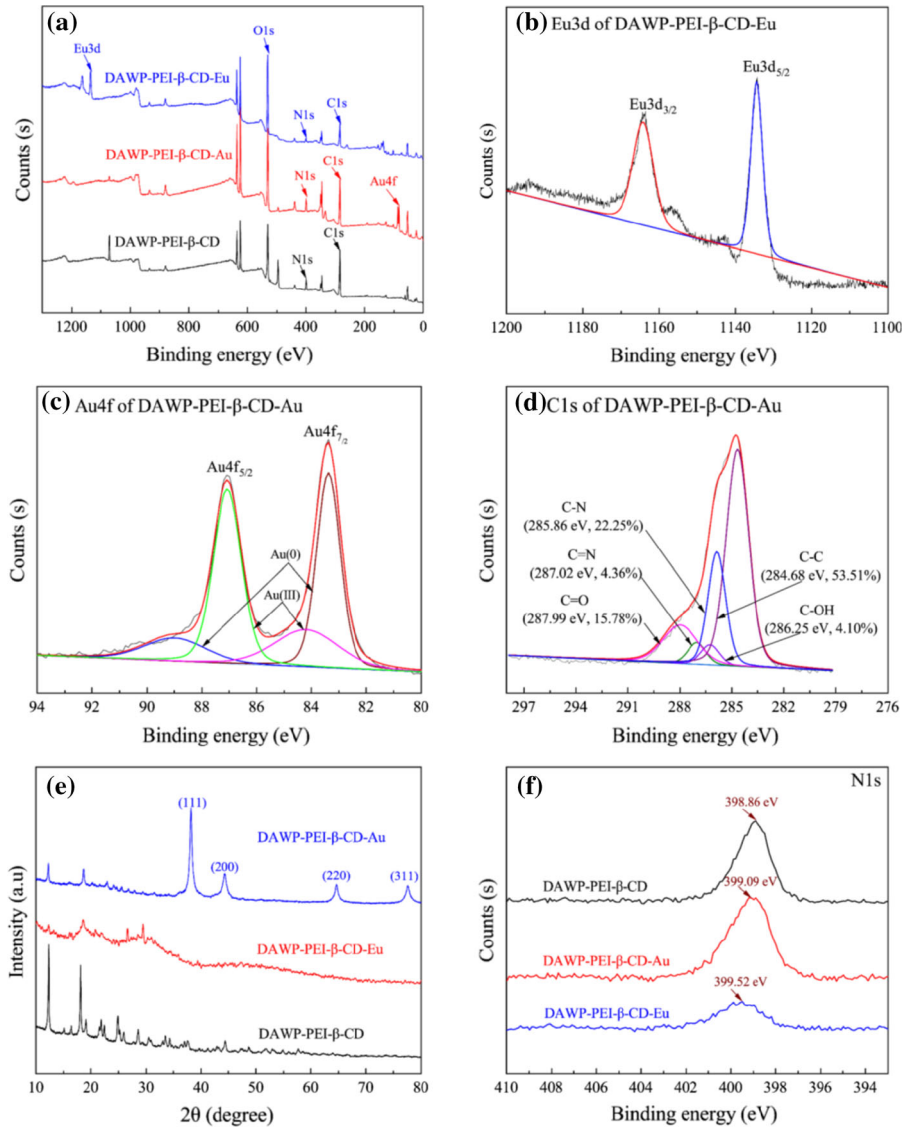

Fig. 8 XPS survey (**a**), Eu3d, Au4f, C1s, N1s spectra (**b**, **c**, **f**) and XRD patterns (**e**) of DAWP-PEI-β-CD, DAWP-PEI-β-CD-Au and DAWP-PEI-β-CD-Eu

processes. Besides, in Fig. 8f, the N1s peaks shifted from 398.86 to 399.09 eV after Au(III) adsorption, while it was shifted from 398.86 to 399.52 eV after Eu(III) adsorption, which illuminated that the nitrogen containing functional groups played roles not only as a cross-linker but also as adsorption sites for Eu(III) and Au(III). On the basis of characterization analysis as well as adsorption experiments, the removal mechanism of the targeted contaminants by DAWP-PEI-β-CD was schematically illustrated in Fig. 9. The elimination mechanism of Eu(III) by DAWP-PEI-β-CD was mainly through the surface coordination and host-guest inclusion interaction. Specifically, on the one hand, the ample amino groups of DAWP-PEI-β-CD that could form complex compounds with Eu(III). On the other hand, the cavities of β-CD could make contributions to the host-guest inclusion complexes with Eu(III). However, the adsorption mechanism of Au(III) on DAWP-PEI-β-CD was mainly attributed to the electrostatic attraction, chelation, host-guest inclusion, and redox reaction. Once the fresh DAWP-PEI-β-CD was exposed to Au(III) solution, the targeted

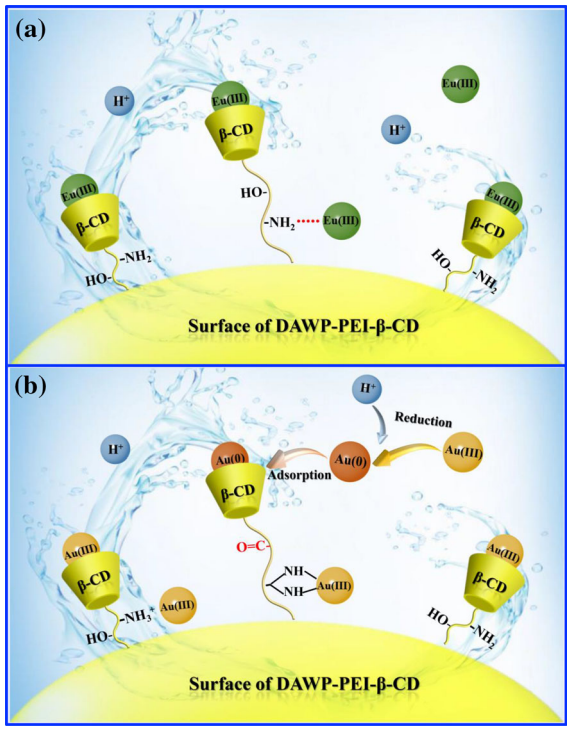

Fig. 9 Schematic diagram of the plausible adsorption mechanism of Eu(III) and Au(III) by DAWP-PEI-β-CD

contaminants were rapidly enriched onto DAWP-PEI-β-CD surface via electrostatic interaction, and followed the reduction of a part of Au(III) to Au(0) with the help of reductive functional groups. Finally, most of Au(III) and Au(0) were immobilized on the surface of DAWP-PEI-β-CD by the host-guest inclusion interaction.

Conclusions

In summary, a novel bio-adsorbent (DAWP-PEI-β-CD) was synthesized by grafting PEI and β-CD into dialdehyde waste paper via a facile two-step method. Characterization results found that the β-CD and amino groups played an important role in uptake of Eu(III) and Au(III). Batch experiment showed that the isotherm and kinetic data were fitted well to the Langmuir and pseudo-second-order models, and the saturated adsorption capacity of Eu(III) (pH=6.0) and Au(III) (pH=2.0) onto DAWP-PEI-β-CD were 424.2 and 241.3 mg/g, respectively. The thermodynamic parameters suggested that the adsorption of Eu(III) and Au(III) on DAWP-PEI-β-CD were a spontaneous and endothermic process. The adsorption mechanism study revealed that the elimination of Eu(III) was attributed to host-guest inclusion and surface complexation interactions, while adsorption of Au(III) might stem from a combination of electrostatic attraction, chelation, host-guest inclusion and oxidation-reduction interaction. Thus, these results will facilitate the development of new type biomass-based materials for Eu(III) and Au(III) pollution cleanup.

Acknowledgments We gratefully thank the Research Fund Program of National Natural Science Foundation of China (No. 21876115), Zhejiang Public Welfare Technology Application and Social Development Project (LGF21C030001), China Postdoctoral Science Foundation (2021M702911) and State Key Laboratory of Pollution Control and Resource Reuse Foundation (No. PCRRF18021).

Author contributions FL, SH: Investigation, Data curation, Writing-original draft. QH, CW: Investigation, Project administration. BH: Writing-review & editing.

Data availability All data are available from the authors upon reasonable request.

Declarations

Conflict of interest There are no conflict of interest do declare.

References

Al-Harahsheha M, AlJarraha M, Alrebakia M, Mayyasb M (2020) Nanoionic exchanger with unprecedented loading capacity of uranium. Sep Purif Technol 238:116423

Chen C, Hu J, Xu D, Tan X, Meng Y, Wang X (2008) Surface complexation modeling of Sr(II) and Eu(III) adsorption onto oxidized multiwall carbon nanotubes. J Colloid Interface Sci 323:33–41

Chen X, Yang X, Xiang Y, Xu L, Liu G (2020) Humic acid derived resin: an efficient adsorbent for Au(III) uptake from aqueous acidic solution. J Chem Eng Data 65:1824–1832

Cheng W, Wan T, Wang X, Wu W, Hu B (2018) Plasma-grafted polyamine/hydrotalcite as high efficient adsorbents for retention of uranium (VI) from aqueous solutions. Chem Eng J 324:103–111

Crini G, French AD, Kainuma K, Szente L, Jane JL (2021) Contributions of dexter french (1918–1981) to cycloamylose/cyclodextrin and starch science. Carbohydr Polym 257:117620

Dai S, Wang N, Qi C, Wang X, Ma Y, Yang L, Liu X, Huang Q, Nie C, Hu B, Wang X (2019) Preparation of core-shell

structure Fe_3O_4@C@MnO_2 nanoparticles for effificient elimination of U(VI) and Eu(III) ions. Sci Total Environ 685:986–996

Fang Q, Duan S, Zhang J, Li J, Leung K (2017) Dual shelled Fe_3O_4/polydopamine hollow microspheres as an effective Eu(III) adsorbent. J Mater Chem A 5:2947–2958

Guo Z, Li Y, Pan S, Xu J (2015) Fabrication of Fe_3O_4 @cyclodextrin magnetic composite for the high-efficient removal of Eu(III). J Mol Liq 206:272–277

Hu B, Wang H, Liu R, Qiu M (2021) Highly efficient U(VI) capture by amidoxime/carbon nitride composites: evidence of EXAFS and modeling. Chemosphere 274:129743

Huang S, Pang H, Li L, Jiang S, Wen T, Zhuang L, Hu B, Wang X (2018) Unexpected ultrafast and high adsorption of U(VI) and Eu(III) from solution using porous Al_2O_3 microspheres derived from MIL-53. Chem Eng J 353:157–166

Liu H, Zhou Y, Yang Y, Zou K, Wu R, Xia K, Xie S (2019a) Synthesis of polyethylenimine/graphene oxide for the adsorption of U(VI) from aqueous solution. Appl Surf Sci 471:88–95

Liu F, Peng G, Li T, Yu G, Deng S (2019b) Au(III) adsorption and reduction to gold particles on cost-effective tannin acid immobilized dialdehyde corn starch. Chem Eng J 370:228–223

Liu F, Wang S, Chen S (2020a) Adsorption behavior of Au(III) and Pd(II) on persimmon tannin functionalized viscose fiber and the mechanism. Int J Biol Macromol 152:1242–1251

Liu F, Zhou L, Wang W, Yu G, Deng S (2020b) Adsorptive recovery of Au(III) from aqueous solution using crosslinked polyethyleneimine resins. Chemosphere 241:125122

Liu F, Zhou Z, Li G (2021a) Persimmon tannin functionalized polyacrylonitrile fiber for highly efficient and selective recovery of Au(III) from aqueous solution. Chemosphere 264:128469

Liu F, Hua S, Zhou L, Hu B (2021b) Development and characterization of chitosan functionalized dialdehyde viscose fiber for adsorption of Au(III) and Pd(II). Int J Biol Macromol 173:457–466

Liu F, Hua S, Wang C, Qiu M, Jin L, Hu B (2021c) Adsorption and reduction of Cr(VI) from aqueous solution using cost-effective caffeic acid functionalized corn starch. Chemosphere 279:130539

Li S, Dong L, Wei Z, Sheng G, Hu B (2020) Adsorption and mechanistic study of the invasive plant-derived biochar functionalized with CaAl-LDH for Eu(III) in water. J Environ Sci 96:127–137

Ma J, Zhao Q, Zhou L, Wen T, Wang J (2019) Mutual effects of U(VI) and Eu(III) immobilization on interpenetrating 3-dimensional MnO_2/graphene oxide composites. Sci Total Environ 695:133696

Martin-Trasanco R, Cao R, Esparza-Ponce HE, Montero-Cabrera ME (2017) Reduction of Au(III) by a β-cyclodextrin polymer in acid medium, a stated unattainable reaction. Carbohydr Polym 175:530–537

Neri G, Cordaro A, Cordaroa SM, Mazzaglia A, Piperno A (2021) PEGylated bis-adamantane carboxamide as guest bridge for graphene poly-cyclodextrin gold nanoassemblies. J Mol Struct 1240:130519

Pestov A, Nazirov A, Modin E, Mironenko A, Bratskaya S (2015) Mechanism of Au(III) reduction by chitosan: comprehensive study with ^{13}C and ^{1}H NMR analysis of chitosan degradation products. Carbohydr Polym 117:70–77

Qiu M, Liu Z, Wang S, Hu B (2020) The photocatalytic reduction of U(VI) into U(IV) by ZIF-8/g-C_3N_4 composites at visible light. Environ Res 11:110349

Rahman NHA, Jaafar NR, Annuar NAS, Rahman RA, Murad AMA, El-Enshasy HA, Illias RM (2021) Efficient substrate accessibility of cross-linked levanase aggregates using dialdehyde starch as a macromolecular cross-linker. Carbohydr Polym 267:118159

Slavgorodska MV, Kyrychenko A (2020) Adsorption behavior of β-cyclodextrin onto gold nanoparticles. J Mol Graph Model 94:107483

Shen H, Zhu G, Yu W, Wu H, Ji H, Shi H, She Y, Zheng Y (2015) Fast adsorption of p-nitrophenol from aqueous solution using β-cyclodextrin grafted silica gel. Appl Surf Sci 356:1155–1167

Sun Y, Chen C, Tan X, Shao D, Li J, Zhao G, Yang S, Wang Q, Wang X (2012) Enhanced adsorption of Eu(III) on mesoporous Al_2O_3/expanded graphite composites investigated by macroscopic and microscopic techniques. Dalton Trans 41:13388–13394

Wang H, Liu Y, Zeng G, Hu X, Hu X, Li T, Li H, Wang Y, Jiang L (2014) Grafting of β-cyclodextrin to magnetic graphene oxide via ethylenediamine and application for Cr(VI) removal. Carbohydr Polym 113:166–173

Wang F, Zhao J, Zhu M, Yu J, Hu Y, Liu H (2015) Selective adsorption-deposition of gold nanoparticles onto monodispersed hydrothermal carbon spherules: a reduction-deposition coupled mechanism. J Mater Chem A 3:1666–1674

Wang M, Cheng W, Wan T, Hu BW, Zhu YL, Song XF, Sun YB (2019) Mechanistic investigation of U(VI) sequestration by zero-valent iron/activated carbon composites. Chem Eng J 362:99–106

Wang J, Wang Y, Wang W, Pen T, Liang J, Li P, Pan D, Fan Q, Wu W (2020) Visible light driven Ti^{3+} self-doped TiO_2 for adsorption-photocatalysis of aqueous U(VI). Environ Pollut 262:114373

Wu Y, Li B, Wang X, Yu S, Pang H, Liu Y, Liu X, Wang X (2019) Magnetic metal-organic frameworks (Fe_3O_4@ZIF-8) composites for U(VI) and Eu(III) elimination: simultaneously achieve favorable stability and functionality. Chem Eng J 378:122105

Yan Z, Huang Q, Wang L, Zhang F (2019) Synthesis of tailored bis-succinamides and comparison of their extractability for U(VI), Th(IV) and Eu(III). Sep Purif Technol 213:322–327

Yang S, Li Q, Chen L, Chen Z, Pu Z, Wang H, Yu S, Hu B, Chen J, Wang X (2019) Ultrahigh sorption and reduction of Cr(VI) by two novel core-shell composites combined with Fe_3O_4 and MoS_2. J Hazard Mater 379:120797

Yin L, Hu B, Zhuang L, Fu D, Li J, Hayat T, Alsaedi A, Wang X (2020) Synthesis of flexible cross-linked cryptomelane-type manganese oxide nanowire membranes and their application for U(VI) and Eu(III) elimination from solutions. Chem Eng J 381:122744

Zhao F, Repo E, Yin D, Meng Y, Jafari S, Sillanpää M (2015a) EDTA-cross-linked βcyclodextrin: an environmentally

friendly bifunctional adsorbent for simultaneous adsorption of metals and cationic dyes. Environ Sci Technol 49:10570–10580

Zhao R, Wang Y, Li X, Sun B, Wang C (2015b) Synthesis of βcyclodextrin-based electrospun nanofiber membranes for highly efficient adsorption and separation of methylene blue. ACS Appl Mater Interfaces 7:26649–26657

Zhao F, Repo E, Meng Y, Wang X, Yin D, Sillanpää M (2016) An EDTA-b-cyclodextrin material for the adsorption of rare earth elements and its application in preconcentration of rare earth elements in seawater. J Colloid Interface Sci 465:215–224

Zhao F, Repo E, Song Y, Yin D, Hammouda SB, Chen L, Kalliola S, Tang J, Tam KC, Sillanpää M (2017) Polyethylenimine-cross-linked cellulose nanocrystals for highly efficient recovery of rare earth elements from water and a mechanism study. Green Chem 19:4816–4828

Zhao B, Yuan L, Wang Y, Duan T, Shi W (2021a) Carboxylated UiO-66 tailored for U(VI) and Eu(III) trapping: from batch adsorption to dynamic column separation. ACS Appl Mater Interfaces 13:16300–16308

Zhao Z, Cheng G, Zhang Y, Han B, Wang X (2021b) Metal-organic-framework based functional materials for uranium recovery: performance optimization and structure/functionality-activity relationships. ChemPlusChem 86:1177–1192

Zhang S, Wang J, Zhang Y, Ma J, Huang L, Yu S, Chen L, Song G, Qiu M, Wang X (2021a) Applications of water-stable metal-organic frameworks in the removal of water pollutants: a review. Environ Pollut 291:118076

Zhang M, Dong Z, Hao F, Xie K, Qi W, Zhai M, Zhao L (2021b) Ultrahigh and selective adsorption of Au(III) by rich sulfur and nitrogen-bearing cellulose microspheres and their applications in gold recovery from gold slag leaching solution. Sep Purif Technol 274:119016

Zhu Y, Wang X, Li Z, Fan Y, Zhang X, Chen J, Zhang Y, Dong C, Zhu Y (2021) Husbandry waste derived coralline-like composite biomass material for efficient heavy metal ions removal. Bioresour Technol 337:125408